

Internal β -Turn Hydration: Crystallographic Evidence and Molecular Dynamics SimulationAlfredo Di Nola,[†] Enrico Gavuzzo,[‡] Fernando Mazza,^{*,‡,§} Giorgio Pochetti,[‡] and Danilo Roccatano[†]*Dipartimento di Chimica, Università "La Sapienza", P.A. Moro 5, 00185 Roma, Istituto di Strutturistica Chimica, CNR, C.P.n. 10, 00016 Monterotondo Stazione, Roma, and Dipartimento di Chimica, V. Vetoio, Università, 67010 L'Aquila, Italy**Received: January 5, 1995; In Final Form: March 17, 1995*[®]

The X-ray structure analysis of the monohydrate phase of the peptide For-Met-Leu- Δ^2 Phe-Phe-OMe has revealed that the type-II β -turn supported by the 4 \rightarrow 1 H-bond, expected for the backbone containing the α,β -unsaturated residue Δ^2 Phe, has been modified by the water molecule. The water prevents the 4 \rightarrow 1 H-bond between Met CO and Phe NH groups, forming a H-bonded bridge between these groups and causing significant modification of the secondary structure. The hydrated β -turn found in the crystal can be an interesting static model useful for the comprehension of the internal hydration mechanism of β -turns, secondary structures largely present in globular proteins, but generally distributed only on their surface. The internal hydration, with a H-bonded water bridge and modification of the secondary structure, differs from the most common external hydration, where the externally bound water does not cause modification of secondary structure. In order to verify whether the internally hydrated β -turn could be found even in solution, a molecular dynamics simulation has been performed. The results show that the two forms, the β -turn with the 4 \rightarrow 1 H-bond and that with the H-bonded water bridge, do not differ substantially in their energy values. Moreover, no high-energy barrier prevents interconversion between the two forms. The internal β -turn hydration presents strong analogies with the internally hydrated helical peptide segments found in oligopeptides and proteins.

I. Introduction

The X-ray structure analysis performed on the monohydrate crystal phase of the peptide For-Met-Leu- Δ^2 Phe-Phe-OMe,¹ containing the (*Z*)-2,3-didehydrophenylalanine (Δ^2 Phe), has revealed that the strong tendency of the α,β -unsaturated residue to induce the type-II β -turn² has been modified by the water molecule. The water prevents the 4 \rightarrow 1 H-bond³ between Met CO and Phe NH groups, forming a H-bonded bridge between these two groups and an additional H-bond with the Phe CO. This conformationally constrained peptide, which is an analog of the chemotactic prototype For-Met-Leu-Phe-OMe,^{4–6} has been designed in order to check whether a folded backbone, possessing the formyl group not engaged in an intramolecular H-bond, could still maintain biological activity. This structural feature has already been related to its biological activity.¹ In this paper we consider the aspects regarding the specific interaction between water and β -turns, since in globular proteins these secondary structures are generally located on the surface exposed to the solvent. Full details of the internally hydrated β -turn together with the analysis of the crystal packing are here reported to comprehend all the interactions favoring the access of the water molecule to the peptide polar sites. A molecular dynamics (MD) simulation has also been performed in order to determine whether the internally hydrated β -turn could be found even in solution and to compare its energy to that of the β -turn with the 4 \rightarrow 1 H-bond.

It will be shown that the internally hydrated β -turn found in the crystal can be an interesting static model useful for the comprehension of the hydration mechanism of a β -turn peptide segment. This model presents strong analogies with the internally hydrated helical peptide segments.

TABLE 1: Crystal Data of For-Met-Leu- Δ^2 Phe-Phe-OMe-H₂O

empirical formula	C ₃₁ H ₄₀ N ₄ O ₆ S·H ₂ O
formula weight	614.7
crystal system	orthorhombic
<i>a</i>	9.447(6) Å
<i>b</i>	12.636(8) Å
<i>c</i>	28.454(14) Å
<i>V</i>	3397(3) Å ³
space group	<i>P</i> 2 ₁ 2 ₁
<i>d_c</i>	1.20 g cm ⁻³
<i>Z</i>	4
<i>F</i> (000)	1312
λ (Cu K α)	1.5418 Å
μ (Cu K α)	1.23 mm ⁻¹
crystal size	0.1 \times 0.3 \times 0.04 mm
2 θ_{\max}	138°
refl. with <i>I</i> > 2.5 σ (<i>I</i>)	2409
<i>R</i> , <i>R_w</i>	0.069, 0.089
large diff in ΔF synthesis	-0.25, +0.35 e Å ⁻¹
<i>S</i>	0.3
observations/parameter	6.1

II. Experimental Section

Crystal Data. Crystals were obtained by slow evaporation of a 1:1 water–methanol mixture in which the tetrapeptide was dissolved. A four-circle SYNTEX P2₁ automatic diffractometer equipped with a graphite monochromator and Cu K α radiation was used for crystal and intensity data measurements. The refined unit-cell parameters, determined by a least-squares fit of the angular setting of 18 reflections in the range 15° < θ < 50°, are given in Table 1. Intensity data were collected by the θ -2 θ technique with a scan speed within the interval 1.5–14.5 deg/min⁻¹ over a range of 1.6°. Background counts were taken for a time equal to half the scan time. Three standard reflections, monitored after every 100 collected reflections, showed only small random deviations from their means. Out of a total of 3469 collected reflections, 2409 had *I* > 2.5 σ (*I*) and were considered observed and used in the calculations.

[†] Università "La Sapienza".[‡] Istituto di Strutturistica Chimica, CNR.[§] Università, L'Aquila.[®] Abstract published in *Advance ACS Abstracts*, May 1, 1995.

Lorentz and polarization corrections were applied, but intensities were not corrected for extinction and absorption.

Structure Solution and Refinement. The structure was solved by direct methods using the program SHELXS 86⁷ and Fourier recycling. The heavy atom positions were refined isotropically, then anisotropically, by the full-matrix least-squares method minimizing the function $\sum w(|F_o| - |F_c|)^2$, where $w = (a + |F_o| + c|F_o|^2)^{-1}$ with a and c equal to $2F_{o(\min)}$ and $2/F_{o(\max)}$, respectively. A difference Fourier map computed at this stage showed two peaks of residual electron density, which were interpreted as due to a minor conformation adopted in the crystal by the terminal part of the Met side chain. The refinement was therefore continued with two sulfur and two methyl groups; 0.6 and 0.4 occupancy factors were assigned to both atoms of each species, respectively. After refinement, the geometry of the disordered atoms is $C_{1\gamma} - S_{1\delta^1} = 1.75$ Å, $S_{1\delta^1} - C_{1\epsilon^1} = 1.70$ Å, $C_{1\gamma} - S_{1\delta^1} - C_{1\epsilon^1} = 95^\circ$, $C_{1\gamma} - S_{1\delta^2} = 1.86$ Å, $S_{1\delta^2} - C_{1\epsilon^2} = 1.79$ Å, $C_{1\gamma} - S_{1\delta^2} - C_{1\epsilon^2} = 98^\circ$. After each cycle of refinement the H atoms were generated at the expected positions with C–H and N–H bond lengths of 1.09 and 1.00 Å, respectively, and thermal isotropic parameters deduced from the carrier atoms. The correction for the real and imaginary parts of the anomalous dispersion was taken into account for the sulfur atom. The final atomic coordinates together with their B_{eq} of the non H atoms are given in Table 2. The scattering factors were taken from ref 8. Valence bond lengths and angles, anisotropic thermal parameters, and observed and calculated structure factors have been deposited as supplementary material. The calculations were carried out on the D.G. ECLIPSE MV/8000 II computer using the package of programs of ref 9.

Molecular Dynamics Simulations. Molecular dynamics simulations were performed with programs from the Groningen molecular simulation (GROMOS) system software package.¹⁰ The applied empirical potential energy function contains terms representing bond angle bending, harmonic dihedral angle bending (out-of-plane, out-of-tetrahedral configuration), sinusoidal dihedral angle torsion, and van der Waals and electrostatic interactions.¹¹ A dielectric permittivity, $\epsilon = 1$, was used. The cutoff radius for the nonbonded interactions was 8 Å. The bond stretching term was not included in the calculation: the SHAKE algorithm¹² was used to constrain bond lengths. The use of constant bond lengths in MD is widely adopted since it allows a longer time step and computational time saving; it was also proved that this approximation does not cause modifications of physical and chemical properties.¹³ The tetrapeptide was immersed in a rectangular box with edges of 20.14, 24.05, and 26.61 Å, containing 292 solvent molecules (water–methanol mixture in a 1:1 molar ratio), subjected to periodic boundary conditions. The starting conformation of the peptide was that found in the monohydrate crystal phase. Weak coupling to an external thermal bath at the desired temperature, with a coupling time constant of 0.1 ps, and to an external pressure bath of 10⁵ Pa with a coupling time constant of 0.5 ps was used to maintain constant temperature and pressure during the simulations.¹⁴ The simple point charge (SPC)¹⁵ model was adopted for water, while the potential model and geometry of the methanol were taken from the *GROMOS Library Manual*.¹⁰ In the MD simulations H-bonds were accepted when the contacts donor–H···acceptor and the angles donor–H···acceptor involved were shorter than 2.5 Å and larger than 125°, respectively. The calculations were performed on the ALPHAs DEC 3000/500 of CASPUR at the University of Rome.

III. Results

Molecular Structure. A perspective view of the crystal conformation together with the adopted numbering scheme is

TABLE 2: Final Fractional Coordinates and B_{eq} (Å²) with esd's in Parentheses for the Non H Atoms

$$B_{eq} = \frac{1}{3} \sum_i \sum_j a_i a_j \beta_{ij}$$

	<i>x</i>	<i>y</i>	<i>z</i>	B_{eq}
C ₀ '	0.3370(7)	−0.0987(6)	0.7399(3)	5.4(2)
O ₀	0.4440(4)	−0.0646(4)	0.7574(2)	6.1(1)
N ₁	0.2069(5)	−0.0781(4)	0.7550(2)	5.0(2)
C ₁ ^α	0.1791(6)	−0.0117(5)	0.7951(2)	4.7(2)
C ₁ ^β	0.2186(9)	−0.0640(6)	0.8423(3)	6.6(2)
C ₁ ^γ	0.131(1)	−0.159(1)	0.8539(5)	11.2(4)
S ₁ ^{δ1a}	0.184(1)	−0.2306(4)	0.9037(2)	11.3(2)
S ₁ ^{δ2b}	0.092(2)	−0.170(1)	0.9177(5)	13.5(5)
C ₁ ^{ε1a}	0.100(5)	−0.151(3)	0.943(1)	16(1)
C ₁ ^{ε2b}	0.270(4)	−0.160(3)	0.939(1)	11.3(9)
C ₁ '	0.2426(6)	0.1004(5)	0.7902(3)	4.4(2)
O ₁	0.3045(5)	0.1423(4)	0.8228(2)	5.7(1)
N ₂	0.2225(5)	0.1447(4)	0.7493(2)	4.2(1)
C ₂ ^α	0.2817(6)	0.2498(4)	0.7377(2)	3.9(1)
C ₂ ^β	0.2894(7)	0.2630(5)	0.6841(2)	4.9(2)
C ₂ ^γ	0.3697(8)	0.1754(7)	0.6593(3)	6.1(2)
C ₂ ^{δ1}	0.5181(9)	0.1612(9)	0.6773(4)	9.0(3)
C ₂ ^{δ2}	0.370(2)	0.199(1)	0.6059(3)	10.1(4)
C ₂ '	0.1888(6)	0.3383(5)	0.7577(2)	3.8(1)
O ₂	0.0636(4)	0.3276(3)	0.7658(2)	4.8(1)
N ₃	0.2550(4)	0.4331(4)	0.7612(2)	3.6(1)
C ₃ ^α	0.1728(5)	0.5268(5)	0.7708(2)	3.7(1)
C ₃ ^β	0.1563(6)	0.6048(5)	0.7395(2)	4.0(1)
C ₃ ^γ	0.2082(6)	0.6108(5)	0.6898(2)	4.3(2)
C ₃ ^{δ1}	0.3448(7)	0.5804(6)	0.6777(3)	5.2(2)
C ₃ ^{δ2}	0.1176(7)	0.6471(6)	0.6561(3)	5.3(2)
C ₃ ^{ε1}	0.3863(8)	0.5848(8)	0.6318(3)	6.5(2)
C ₃ ^{ε2}	0.1544(9)	0.6473(8)	0.6098(3)	6.9(3)
C ₃ ^ε	0.292(1)	0.6166(8)	0.5973(3)	6.9(2)
C ₃ '	0.1015(6)	0.5335(5)	0.8163(2)	4.0(2)
O ₃	−0.0116(5)	0.5834(4)	0.8213(2)	5.5(1)
N ₄	0.1657(6)	0.4889(4)	0.8532(2)	4.7(1)
C ₄ ^α	0.1024(9)	0.4890(6)	0.8990(2)	5.5(2)
C ₄ ^β	0.0228(9)	0.3830(7)	0.9075(3)	6.1(2)
C ₄ ^γ	−0.0779(9)	0.3845(8)	0.9490(3)	6.5(2)
C ₄ ^{δ1}	−0.047(1)	0.3400(9)	0.9906(3)	8.4(3)
C ₄ ^{δ2}	−0.210(1)	0.425(1)	0.9438(5)	11.1(5)
C ₄ ^{ε1}	−0.145(2)	0.339(1)	1.0276(4)	10.6(5)
C ₄ ^{ε2}	−0.307(2)	0.430(1)	0.9777(7)	13.9(7)
C ₄ ^ε	−0.275(2)	0.386(1)	1.0198(7)	13.5(7)
C ₄ '	0.217(1)	0.5063(8)	0.9355(3)	6.9(3)
O ₄	0.335(1)	0.474(1)	0.9314(3)	12.8(4)
O ₄ '	0.172(1)	0.5565(6)	0.9716(2)	10.5(3)
C ₅	0.271(3)	0.581(1)	1.0087(4)	18(1)
O _w	0.4174(8)	0.3400(5)	0.8503(2)	8.6(2)

^a An occupancy factor of 0.6 was assigned to this atom during the refinement. ^b An occupancy factor of 0.4 was assigned to this atom during the refinement.

reported in Figure 1, while the relevant backbone and side-chain torsion angles are reported in Table 3. Considering that α, β -unsaturated residues are strong inducers of type-II β -turns when inserted at (i+1) or (i+2) corner positions² and that the Δ^2 Phe is the (i+2)th term because of its penultimate position, the 4 → 1 H-bond acceptor should involve the Met CO group, leaving the For CO free from intramolecular H-bonding. In the crystal, the Δ^2 Phe residue induces backbone folding in the form of an unexpected "open turn" described by the following torsion angles: $\varphi_1 = 57.2^\circ$, $\psi_1 = 44.7^\circ$, $\varphi_2 = -81.1^\circ$, $\psi_2 = 161.2^\circ$, $\varphi_3 = 65.2^\circ$, $\psi_3 = 33.4^\circ$, $\varphi_4 = -141.6^\circ$, $\psi_4 = 148.3^\circ$. Helical and extended conformations occur at the N- and C-terminal residues, respectively, while the φ and ψ of the two central residues deviate significantly from those of the type-II β -turn (-60° , 120° , 80° , 0°).³ Such deviations, the largest one being 41° for ψ_2 , allow the penetration of the water molecule into the backbone loop, where it forms three H-bonds with the Met CO and with the Phe NH and CO groups, respectively. The

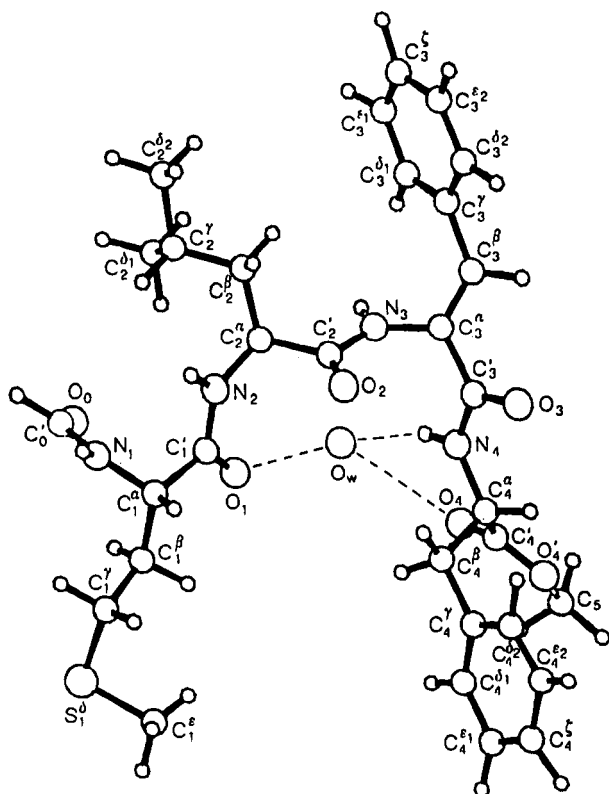


Figure 1. Perspective view of the crystal conformation of the monohydrate tetrapeptide.

water, bridging the Met CO and Phe NH groups by two H-bonds, prevents their $4 \rightarrow 1$ H-bond; the distance $O_1 \cdots N_4$ is 4.65 Å. Moreover, the distance $C_1^\alpha \cdots C_4^\alpha$ of the terminal Met and Phe residues is 7.02 Å, a limiting value for considering the backbone segment as a turn.¹⁶

The formamido group presenting the two H atoms in cis configuration, as usually found in the *N*-formylpeptide crystal structures,^{17–20} is completely planar ($\omega_0 = 0^\circ$). The other three peptide bonds are trans-planar, and, among them, the Leu- Δ^2 -Phe junction presents the largest deviation from planarity ($\omega = 168.2^\circ$). The Met side-chain atoms with higher and lower occupancy factors adopt the g^-, t, g^+ and g^-, t, g^- conformations, respectively. The *t* conformation more frequently occurs for χ^3 in the oligopeptide structures of unbranched side-chain residues.²¹ The Leu side chain assumes the most frequently occurring $g^-(t, g^-)$ conformation.^{21,22} The Δ^2 Phe side chain with $\chi^{2,1} = -44.1^\circ$ and $\chi^{2,2} = 135.8^\circ$ shows the largest deviation from planarity among the Δ^2 Phe-containing oligopeptide crystal

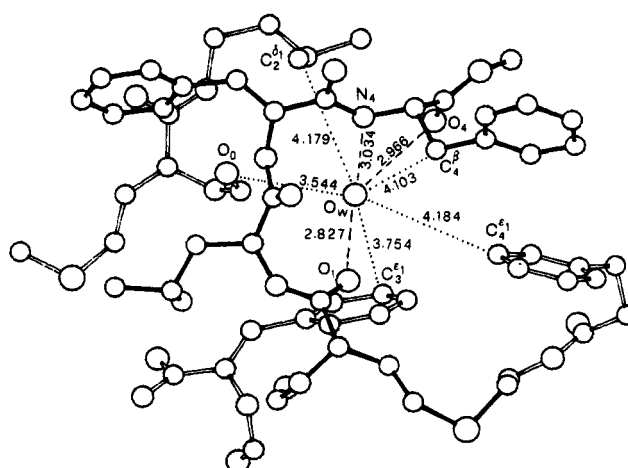


Figure 2. Interactions that the water oxygen forms with the atoms of the surrounding molecules. Dashed and dotted lines represent the H-bonds and the shortest contacts, respectively. The reference molecule is represented by full bonds, whereas, for clarity, the surrounding ones are shown only in part. The asymmetric units are indicated in the text.

structures.² Moreover, the torsion angles $C_2' - N_3 - C_3^\alpha - C_3^\beta$ and $O_3 - C_3' - C_3^\alpha - C_3^\beta$, respectively of -112.7° and 27.9° , indicate that the α, β double bond could conjugate to a larger extent with the carbonyl group rather than with the enamidic nitrogen N_3 . Therefore, conjugation should be allowed from the α, β double bond to the carbonylic oxygen and should scarcely involve the aromatic ring and the enamidic nitrogen N_3 . In accordance, the alteration of bond lengths is practically limited to the $C_3^\alpha - C_3'$ (1.464 Å) and $C_3' - O_3$ (1.248 Å) bonds, respectively shorter and longer than the standard values of saturated models, while the $C_3^\beta - C_3^\gamma$ bond length (1.498 Å) is not significantly altered. The Phe χ^1 is trans, while the χ^2 is in the usual conformation centered around $\pm 90^\circ$.^{21–23}

Crystal Packing. The H-bonds and the shortest contacts between the water oxygen and the atoms of the surrounding molecules are shown in Figure 2. The water forms three H-bonds with the Met CO (2.827 Å) and with the Phe NH (3.034 Å) and CO (2.966 Å) groups of the same molecule. The water H atoms, not detected in the final Fourier map, should not be too far from the $O \cdots O_w$ directions, since the angle $O_1 \cdots O_w \cdots O_4$ is 128° . Additional dipole–dipole interactions may occur between water and the Leu- Δ^2 Phe amide junction; the angle between the plane of the amide and that containing the O_1, O_4, O_w atoms is 39° . The shortest contacts are formed with the methylenic C_4^β atom (4.103 Å) of the reference molecule, with the formylic O_6 (3.544 Å) and the Leu methyl $C_2^{\delta 1}$ (4.179 Å)

TABLE 3: Relevant Torsion Angles (deg) with Estimated Standard Deviations in Parentheses of the Monohydrate Tetrapeptide

backbone			side chain			
$O_0 - C_0' - N_1 - C_1^\alpha$	ω_0	0(1)	Met	$N_1 - C_1^\alpha - C_1^\beta - C_1^\gamma$	χ_1^1	-65.2(9)
$C_0' - N_1 - C_1^\alpha - C_1'$	φ_1	57.2(8)		$C_1^\alpha - C_1^\beta - C_1^\gamma - S_1^{\delta 1}$	$\chi_1^{2,1}$	173.1(7)
$N_1 - C_1^\alpha - C_1' - N_2$	ψ_1	44.7(7)		$C_1^\alpha - C_1^\beta - C_1^\gamma - S_1^{\delta 2}$	$\chi_1^{2,2}$	-143.7(9)
$C_1^\alpha - C_1' - N_2 - C_2^\alpha$	ω_1	-177.2(5)		$C_1^\beta - C_1^\gamma - S_1^{\delta 1} - C_1^{\epsilon 1}$	$\chi_1^{3,1}$	83(2)
$C_1' - N_2 - C_2^\alpha - C_2'$	φ_2	-81.1(6)		$C_1^\beta - C_1^\gamma - S_1^{\delta 2} - C_1^{\epsilon 2}$	$\chi_1^{3,2}$	-52(2)
$N_2 - C_2^\alpha - C_2' - N_3$	ψ_2	161.2(5)	Leu	$N_2 - C_2^\alpha - C_2^\beta - C_2^\gamma$	χ_2^1	-54.5(7)
$C_2^\alpha - C_2' - N_3 - C_3^\alpha$	ω_2	168.2(5)		$C_2^\alpha - C_2^\beta - C_2^\gamma - C_2^{\delta 1}$	$\chi_2^{2,1}$	-56.1(9)
$C_2' - N_3 - C_3^\alpha - C_3'$	φ_3	65.2(7)		$C_2^\alpha - C_2^\beta - C_2^\gamma - C_2^{\delta 2}$	$\chi_2^{2,2}$	-179.5(7)
$N_3 - C_3^\alpha - C_3' - N_4$	ψ_3	33.4(8)	Δ^2 Phe	$N_3 - C_3^\alpha - C_3^\beta - C_3^\gamma$	χ_3^1	3.4(9)
$C_3^\alpha - C_3' - N_4 - C_4^\alpha$	ω_3	-178.3(6)		$C_3^\alpha - C_3^\beta - C_3^\gamma - C_3^{\delta 1}$	$\chi_3^{2,1}$	-44.1(9)
$C_3' - N_4 - C_4^\alpha - C_4'$	φ_4	-141.6(7)		$C_3^\alpha - C_3^\beta - C_3^\gamma - C_3^{\delta 2}$	$\chi_3^{2,2}$	135.8(7)
$N_4 - C_4^\alpha - C_4' - O_4'$	ψ_T	148.3(8)		$C_2' - N_3 - C_3^\alpha - C_3^\beta$		-112.7(6)
$C_4^\alpha - C_4' - O_4' - C_5$		-179(1)		$O_3 - C_3' - C_3^\alpha - C_3^\beta$		27.9(9)
$O_4 - C_4' - O_4' - C_5$		3(1)	Phe	$N_4 - C_4^\alpha - C_4^\beta - C_4^\gamma$	χ_4^1	-165.4(7)
				$C_4^\alpha - C_4^\beta - C_4^\gamma - C_4^{\delta 1}$	$\chi_4^{2,1}$	-103(1)
				$C_4^\alpha - C_4^\beta - C_4^\gamma - C_4^{\delta 2}$	$\chi_4^{2,2}$	82(1)

TABLE 4: Geometric Details of the H-Bonds Found in the Crystal of the Monohydrate Tetrapeptide^a

donor	acceptor	N-H (Å)	H···A (Å)	D···A (Å)	D-H···A (deg)	N···O=C' (deg)
N ₁	O ₂ ^{lb}	1.00	1.96	2.881	151	141.3
N ₂	O ₃ ^l	1.00	1.98	2.934	158	129.6
N ₃	O ₀ ^{llc}	1.00	1.90	2.892	172	138.2
N ₄	O _w	1.00	2.09	3.034	158	
O _w	O ₁			2.827		
O _w	O ₄			2.966		

^a Estimated standard deviations are in the range 0.006–0.01 Å for the contacts and 0.6–1.0° for the angles, respectively. ^b I: $-x, y-1/2, 2/3-z$. ^c II: $-x+1, 1/2+y, 3/2-z$.

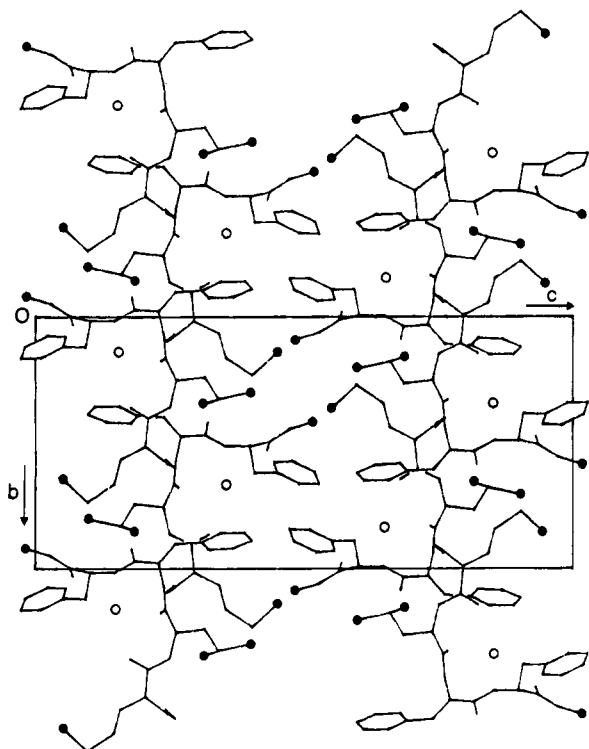


Figure 3. Projection of the crystal packing on the b,c plane. Full and empty circles represent methyl groups and water oxygens, respectively.

of the molecule at $1-x, y+1/2, 3/2-z$, and with the aromatic atoms C₃^{ε1} (3.754 Å) at $1-x, y-1/2, 3/2-z$ and C₄^{ε1} (4.184 Å) at $1/2+x, 1/2-y, 2-z$.

The peptide molecules pack together by three intermolecular H-bonds that the Met, Leu, and Δ²Phe NH groups form with the Leu, Δ²Phe, and For carbonyl oxygens, respectively. Their relevant parameters are reported in Table 4. A projection of the crystal packing on the b,c plane is shown in Figure 3. The packing is completed by van der Waals interactions mainly involving the aromatic and methyl groups of the hydrophobic side chains of different molecules. The shortest contacts among aromatic–aromatic, methyl–methyl, and aromatic–methyl carbon atoms are 3.508, 3.514, and 3.595 Å, respectively, for the couples of atoms C₄^γ···C₃^{ε3} at $-x, y-1/2, 3/2-z$, C₁^{ε1}···C₅ at $x-1/2, 1/2-y, 2-z$, and C₃^{ε5}···C₅ at $1/2-x, 1-y, z-1/2$.

MD Simulation. In order to check whether the tetrapeptide conformation with the water molecule H-bonding the CO_i and NH_{i+3} groups (CO_i···O_w···NH_{i+3}) could be found, at least in part, even in solution, a MD simulation was performed in a 1:1 molar ratio water–methanol mixture at 298 K. The crystal conformation was initially adopted for the tetrapeptide.

The occurrence of the H-bonds involving both CO_i and NH_{i+3} groups during the 100 ps of MD simulation is reported in Figure 4. In the first part of the simulation, up to 60 ps, a water

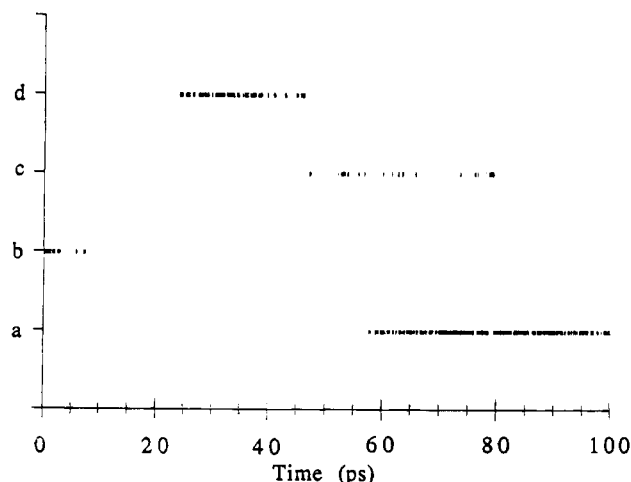


Figure 4. Occurrence of H-bonds involving the CO_i and NH_{i+3} groups of the tetrapeptide during the 100 ps of the MD simulation in the water–methanol mixture at 298 K: (a) CO_i···NH_{i+3}; (b) CO_i···O₁₄₆···NH_{i+3}; (c) CO_i···O₁₈₉···NH_{i+3}; (d) CO_i···O₂₃₈···NH_{i+3}. O₁₄₆, O₁₈₉, and O₂₃₈ represent three different water molecules. When no H-bond is reported, the polar groups of the solute are externally H-bonded to solvent molecules.

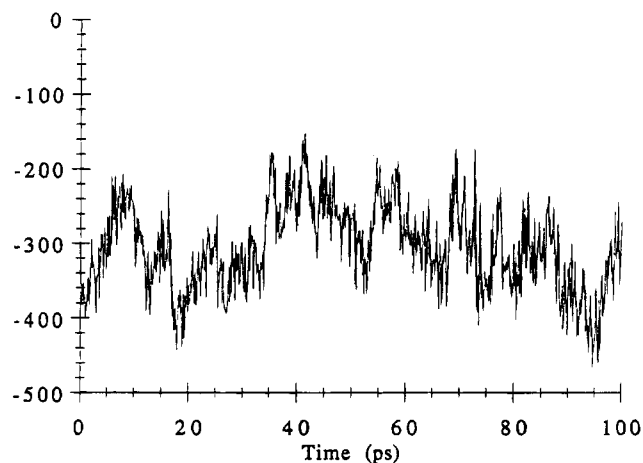


Figure 5. Total potential energy (kJ mol⁻¹, ordinate) of the peptide solute during the 100 ps of the MD simulation in the water–methanol mixture at 298 K.

molecule bridges the CO_i and NH_{i+3} groups, by two H-bonds. However, at least three different water molecules alternate in sequence, showing a fast exchange process. After 60 ps, the 4 → 1 H-bond (CO_i···NH_{i+3}) supporting the β-turn conformation takes place for the remainder of the simulation. The potential energy of the solute during the 100 ps of simulation is reported in Figure 5. The large fluctuations and the reduced length of simulation do not allow quantitative analysis of energy differences; however, the energy values occurring in correspondence with conformations with a H-bonded water bridge (CO_i···O_w···NH_{i+3}) or a 4 → 1 H-bond (CO_i···NH_{i+3}) do not differ substantially and no high-energy barrier prevents conversion between these two forms. The dynamical behavior of the distance MetC₁^α···PheC₄^α during the 100 ps of simulation is reported in Figure 6. The separation between the hydrophobic side chains of these terminal residues plays a relevant role for the access of the water to the central polar sites of the peptide backbone. A large separation favored, as in the crystal, by interactions among the hydrophobic side chains of adjacent molecules allows the entry of the water molecule and the successive formation of an H-bonded water bridge. The lack of such hydrophobic intermolecular interactions, as in solution,

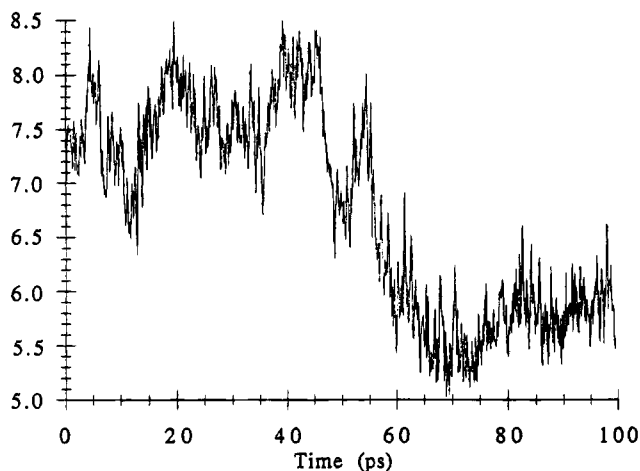


Figure 6. Dynamical behavior of the MetC₁^α...PheC₄^α distance (Å, ordinate) of the tetrapeptide during the 100 ps of the MD simulation in the water–methanol mixture at 298 K.

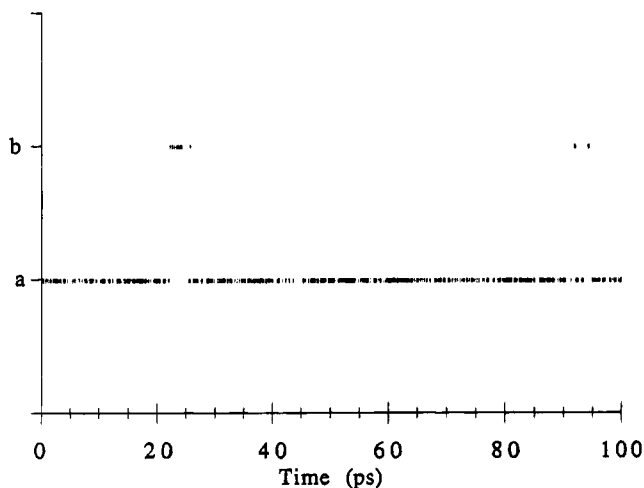


Figure 7. Occurrence of H-bonds involving the CO_{*i*} and NH_{*i*+3} groups of the tetrapeptide during an additional 100 ps of MD simulation in the water–methanol mixture at 310 K: (a) CO_{*i*}...NH_{*i*+3}; (b) CO_{*i*}...O₁₇₃...NH_{*i*+3}. O₁₇₃ represents a water molecule. When no H-bond is reported, the polar groups of the solute are externally H-bonded to solvent molecules.

favors a closer approach of Met and Phe side chains and the 4 → 1 H-bond formation preventing the water molecule insertion.

In order to check the reversibility of the conversion between the conformations containing (CO_{*i*}...O_w...NH_{*i*+3}) and (CO_{*i*}...NH_{*i*+3}) H-bonds, the simulation was continued for an additional 100 ps at a slightly higher temperature (310 K). The temperature was raised to increase the conformational search of the simulation. The occurrence of the H-bonds involving both CO_{*i*} and NH_{*i*+3} groups during the second MD simulation is reported in Figure 7. The (CO_{*i*}...NH_{*i*+3}) H-bond supporting the β -turn is present for about 60% of the time, whereas for about 2% the (CO_{*i*}...O_w...NH_{*i*+3}) H-bonded bridge mediated by the water molecule appears. Figure 8 shows the superposition of the crystal conformation with that internally hydrated obtained at $t = 23$ ps during the last MD simulation. The similarity can be noted not only for the backbones but also for the side chains. From MD simulations it can be concluded that in solution the β -turn appears more stable, but, even if with low probability, it can reversibly accommodate the water molecule that bridges the CO_{*i*} and NH_{*i*+3} groups, with modification of secondary structure. In the crystal the “open turn” is favored by the hydrophobic intermolecular interactions not present in solution.

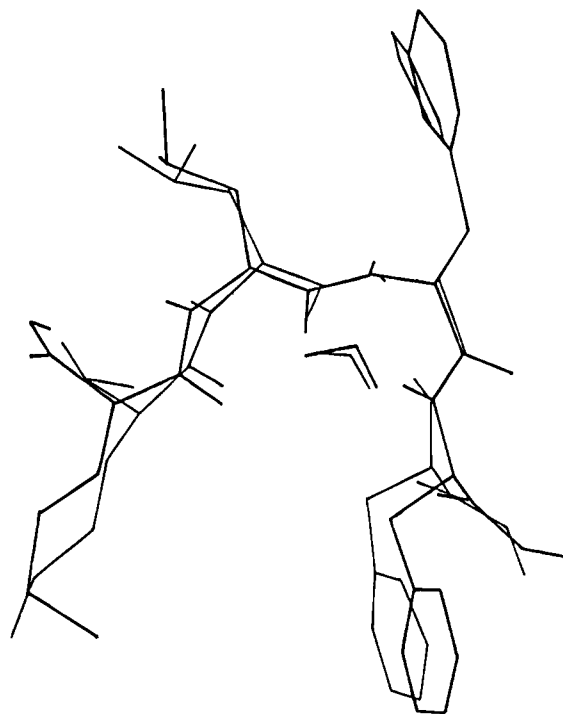


Figure 8. Superposition of the tetrapeptide crystal conformation (thick lines) to that internally hydrated obtained at $t = 23$ ps during the last MD simulation (thin lines). For clarity only the H atoms of the backbones have been reported.

IV. Discussion

The present study furnishes further insights on the influence of the approach of the water molecule to a peptide conformation and on the mechanism of hydration of a secondary structure, problems which cannot be easily determined by spectroscopic techniques.

Although several examples of folded peptide sequences in which water molecules are H-bonded to external polar sites are reported, a water–peptide interaction similar to the present one has been found in the monohydrate crystal form of *t*-Bu-CO-Pro-Me-D-Ala-NHMe.²⁴ This is reported as the first case of a conformation folded by interaction with a water molecule included in a loop containing 12 atoms and described by the following torsion angles: $\varphi_1 = -68.6^\circ$, $\psi_1 = 164.3^\circ$, $\varphi_{i+1} = 138.6^\circ$, $\psi_{i+1} = -35.0^\circ$. In analogy with our case, the water bridges the *tert*-butyl carbonyl group and the C-terminal methylamide NH, by two H-bonds, preventing the 4 → 1 H-bond characteristic of the β -turn and causing modification of secondary structure. At variance, the water forms a third H-bond with the Me-D-Ala CO group of a neighboring molecule, giving rise to a H-bonding network involving both intra- and interturn interactions. The same authors have also shown that the anhydrous crystal form of the peptide adopts the type-II β -turn with the 4 → 1 H-bond and torsion angles $\varphi_i = -58^\circ$, $\psi_i = 136^\circ$, $\varphi_{i+1} = 97^\circ$, and $\psi_{i+1} = -19^\circ$.

Intra- and intermolecular H-bonded water bridges have also been observed in the crystal of (benzyloxycarbonyl)alanyl-D-phenylalanylproline monohydrate,²⁵ where the water bridges two terminal oxygens, and in the crystal of the tri- α -aminoisobutyric acid dihydrate,²⁶ where the amino and carbonyl groups of the first and second residue are respectively H-bonded to the two water molecules connected by an internal H-bond bridge.

A further interesting aspect concerning the specific interaction between water and β -turns comes from the observation that, in globular proteins, these secondary structures are generally located on the surface, which is exposed to the solvent. On

the basis of an investigation of 938 β -turns extracted from the X-ray structures of 58 proteins at a resolution ≤ 2 Å, it has been shown that about 60% of the examined turns had deformations of $\pm 30^\circ$ around the expected φ and ψ values, with a further flexibility of an angle to deviate by as much as $\pm 45^\circ$.²⁷ These deformations are comparable to those found in the crystal of the monohydrate tetrapeptide; therefore, the "open turn" stabilized by the H-bonding network of the water molecule could also be an interesting static model for the comprehension of the hydration mechanism of type-II β -turn backbones containing apolar side chains.

A simpler mode of β -turn hydration has already been proposed on the basis of the crystal structure of the dihydrated form of cyclo[Gly-Pro-Ser-Gly-(δ)Ava] containing the Pro-Ser subunit frequently found in β -turns of globular proteins. The backbone torsion angles of this subunit ($\varphi_{\text{Pro}} = -63.3^\circ$, $\psi_{\text{Pro}} = 23.2^\circ$, $\varphi_{\text{Ser}} = -96.3^\circ$, $\psi_{\text{Ser}} = 4.8^\circ$)²⁸ are very close to those expected for the type-I β -turn (-60° , -30° ; -90° , 0°);³ the CO and NH of the peptide group linking the two chiral residues are respectively H-bonded to each of the two water molecules. A H-bonding network in the form of a water-water-amide polymer takes place in the crystal. In this case the water is externally bound and does not cause $4 \rightarrow 1$ H-bond rupture or significant modification of secondary structure.

Both models of β -turn hydration, either internal with a H-bonded water bridge and modification of secondary structure, as in the case of the tetrapeptide, or external, without modification of secondary structure, as in the case of the cyclopeptide,²⁸ show tight analogies with the hydration of helical peptide segments occurring in oligopeptides and proteins.

The crystal structure of the internally hydrated helical decapeptide Boc-(Aib-Ala-Leu)₃-Aib-OMe²⁹ indicates that the water opens the helix H-bond between Ala² CO and Ala⁵ NH groups, causing a N \cdots O separation of 5.05 Å. At variance with the internally hydrated tetrapeptide, here the secondary structure is distorted only at the φ , ψ values of Leu³, changing from -75° , -42° for the normal to -102° , 15° for the hydrated helix. This distortion, which exposes the Aib¹ CO to an additional water, forming a minisolvation region with the first one, confers amphiphilic character to a peptide containing all apolar residues.

The crystal structure of Boc-Val-Ala-Leu-Aib-Val-Ala-Leu-OMe³⁰ contains two independent molecules in the asymmetric unit. One is completely helical, whereas the helix of the other one is internally hydrated by a water bridging the Leu³ CO and Leu⁷ NH groups with two H-bonds. Also in this case the secondary structure is distorted only at the φ , ψ values of Val⁵, changing from -87° , -11° before to -91° , 2° after hydration. It is interesting to note the occurrence of both normal and internally hydrated helices in the same crystal, indicating that the conversion from anhydrous to hydrated helix should be a facile process. This observation is in agreement with the potential energy computed for the tetrapeptide during the MD simulation, showing that the two β -turn forms containing (CO_i \cdots NH_{i+3}) and (CO_i \cdots O_w \cdots NH_{i+3}) H-bonds do not differ substantially in their energy values.

In protein crystal structures, the α -helices are often hydrated, either externally by a water H-bonding to the backbone carbonyl oxygen or internally by a water inserting into the helix H-bond and forming a H-bonded bridge between the backbone CO and NH groups. The hydration with externally bound water, without modification of secondary structure, seems the most common case. In fact from an analysis of 312 hydrated α -helical segments extracted from 35 protein structures refined at ≤ 1.9 Å,³¹ it resulted that 262 had externally bound water with $5 \rightarrow 1$ and CO_i \cdots O_w H-bonds, 33 had internally bound water with

(CO_i \cdots O_w \cdots NH_{i+4}) H-bonds, and 17 were three-center transition states with $5 \rightarrow 1$ and (CO_i \cdots O_w \cdots NH_{i+4}) H-bonds. The water-inserted segments show considerable conformational diversity, depending on the degree of penetration of the water molecule into the helical segment and could represent trapped intermediates in the unfolding-folding process of α -helices. A "conformational reaction coordinate" of the progressive unfolding of the α -helix has been represented by water-inserted segments differing little in conformation and, therefore, in energy.³¹

The mechanism by which secondary structural elements of proteins are made, broken, or interconverted is of considerable interest,³² and in principle it can be studied by MD simulation. Folding and unfolding processes have been observed in dynamics simulations;³³⁻³⁵ however, very few examples are reported in the literature on the internal hydration of secondary structures. Soman et al.³³ have studied the unfolding of an α -helix fragment of myoglobin composed of 18 residues. This unfolds with a variety of mechanisms; one of them consists of the insertion of a water molecule into an internal H-bond. An analogous behavior was found by Di Capua et al.³⁶ in the case of polyalanine.

V. Conclusion

The crystal and molecular structure of the monohydrate phase of the tetrapeptide has shown the conformational modification of the peptide backbone caused by the internally H-bonded water molecule; the access of water to the peptide polar sites is favored by interactions among apolar side chains of neighboring molecules. A MD simulation has shown that the internally hydrated β -turn can be found also in solution, and its potential energy does not differ substantially from that of the β -turn with a $4 \rightarrow 1$ H-bond.

Moreover, the interconversion between the two forms can reversibly take place. Therefore, the internally hydrated crystal form can be a static model useful for understanding the mechanism of internal hydration of β -turn peptide segments.

Internally hydrated β -turn and helical peptide segments present strong analogies. They can be summarized as follows: the access of water to the polar sites of the backbone causes $4 \rightarrow 1$ and $5 \rightarrow 1$ H-bond rupture for the β -turn and helical segment, respectively. H-bonded water bridges of the type (CO_i \cdots O_w \cdots NH_{i+3}) for the β -turn and (CO_i \cdots O_w \cdots NH_{i+4}) for the α -helix, respectively, are formed. The deformation of secondary structure involves the φ and ψ backbone torsion angles of both central residues of the β -turn and even of only one residue in the case of the helical segment. In both cases the largest deviations observed for these angles are ± 40 – 50° .

Acknowledgment. The work has been partly supported by MURST. Drawings by Mr. Trabassi.

Supplementary Material Available: Valence bond lengths and angles with esd's and anisotropic thermal parameters with esd's (4 pages); observed and calculated structure factors (12 pages). Ordering information is given on any current masthead page.

References and Notes

- (1) Torrini, I.; Pagani Zecchini, G.; Paglialonga Paradisi, M.; Lucente, G.; Gavuzzo, E.; Mazza, F.; Pochetti, G.; Spisani, S. *Tetrahedron* **1993**, *49*, 489.
- (2) Singh, T. P.; Narula, P.; Patel, H. C. *Acta Crystallogr.* **1990**, *B46*, 539.
- (3) Venkatachalam, C. *Biopolymers* **1968**, *6*, 1425.
- (4) Schiffmann, E.; Corcoran, B.; Wahl, S. *Proc. Natl. Acad. Sci. U.S.A.* **1975**, *72*, 1059.

- (5) Showell, H. J.; Freer, R. J.; Zigmond, S. H.; Schiffmann, E.; Aswanikumar, S.; Corcoran, B.; Becker, E. L. *J. Exp. Med.* **1976**, *143*, 1154.
- (6) Freer, R. J.; Day, A. R.; Radding, J. A.; Schiffmann, E.; Aswanikumar, S.; Showell, H. J.; Becker, E. L. *Biochemistry* **1980**, *19*, 2404.
- (7) Sheldrick, G. M. *SHELXS86 Program for the Solution of Crystal Structures*; University of Göttingen: Germany, 1986.
- (8) *International Tables for X-Ray Crystallography*; 2nd ed.; The Kynoch Press: Birmingham, 1974; Vol. IV.
- (9) Camalli, M.; Capitani, D.; Cascarano, G.; Cerrini, S.; Giacobozzo, C.; Spagna, R. *SIR-CAOS (It.Pat.n 35403c/86): User Guide*; Istituto di Strutturistica Chimica, CNR, C.P.n. 10, 00016 Monterotondo Stazione, Roma, Italy.
- (10) van Gunsteren, W. F.; Berendsen, H. J. C. *Groningen Molecular Simulation (GROMOS) Library Manual*; Biomos: Groningen, 1987.
- (11) Aqvist, J.; van Gunsteren, W. F.; Leijonmarck, M.; Tapia, O. *J. Mol. Biol.* **1985**, *183*, 461.
- (12) Ryckaert, J. P.; Ciccotti, G.; Berendsen, H. J. C. *J. Comput. Phys.* **1977**, *23*, 327.
- (13) Karplus, M.; van Gunsteren, W. F. *Macromolecules* **1982**, *15*, 1528.
- (14) Berendsen, H. J. C.; Postma, J. P. M.; van Gunsteren, W. F.; Di Nola, A.; Haak, J. R. *J. Chem. Phys.* **1984**, *81*, 3684.
- (15) Berendsen, H. J. C.; Postma, J. P. M.; van Gunsteren, W. F.; Hermans, J. *Intermolecular Forces*; Pullman, B., Ed.; Reidel: Dordrecht, 1981; p 331.
- (16) Rose, G. D.; Gierasch, L. M.; Smith, J. A. *Adv. Protein Chem.* **1985**, *37*, 1.
- (17) Dentino, A. R.; Raj, P. A.; Bhandary, K. K.; Wilson, M. E.; Levine, M. J. *J. Biol. Chem.* **1991**, *266*, 18460.
- (18) Torrini, I.; Pagani Zecchini, G.; Paglialunga Paradisi, M.; Lucente, G.; Gavuzzo, E.; Mazza, F.; Pochetti, G.; Spisani, S.; Giuliani, A. L. *Int. J. Peptide Protein Res.* **1991**, *38*, 495.
- (19) Pagani Zecchini, G.; Paglialunga Paradisi, M.; Torrini, I.; Lucente, G.; Gavuzzo, E.; Mazza, F.; Pochetti, G.; Paci, M.; Sette, M.; Di Nola, A.; Veglia, G.; Traniello, S.; Spisani, S. *Biopolymers* **1993**, *33*, 437.
- (20) Torrini, I.; Pagani Zecchini, G.; Paglialunga Paradisi, M.; Lucente, G.; Gavuzzo, E.; Mazza, F.; Pochetti, G.; Traniello, S.; Spisani, S.; Cerichelli, G. *Biopolymers* **1994**, *34*, 1291.
- (21) Benedetti, E.; Morelli, G.; Némethy, G.; Scheraga, H. A. *Int. J. Peptide Protein Res.* **1983**, *22*, 1.
- (22) Gould, R. O.; Gray, A. M.; Taylor, P.; Walkinshaw, M. D. *J. Am. Chem. Soc.* **1985**, *107*, 5921.
- (23) Ashida, T.; Tsunogae, Y.; Tanaka, I.; Yamane, T. *Acta Crystallogr.* **1987**, *B43*, 212.
- (24) Aubry, A.; Vitou, B.; Boussard, G.; Marraud, M. *Int. J. Peptide Protein Res.* **1981**, *18*, 195.
- (25) Nair, C. M. K.; Nagaraj, R.; Ramaprasad, S.; Balam, P.; Vijayan, M. *Acta Crystallogr.* **1981**, *B37*, 597.
- (26) Jayashree, A. N.; Suresh, C. G.; Vijayan, M. *Acta Crystallogr.* **1987**, *C43*, 1618.
- (27) Wilmot, C. M.; Thornton, J. M. *Protein Eng.* **1990**, *3*, 479.
- (28) Perczel, A.; Hollosi, M.; Foxman, B. M.; Fasman, G. D. *J. Am. Chem. Soc.* **1991**, *113*, 9772.
- (29) Karle, I. L.; Flippen-Anderson, J.; Uma, K.; Balam, P. *Proc. Natl. Acad. Sci. U.S.A.* **1988**, *85*, 299.
- (30) Karle, I. L.; Balam, P. *Biochemistry* **1990**, *29*, 6747.
- (31) Sundaralingam, M.; Sekharudu, Y. C. *Science* **1989**, *244*, 1333.
- (32) Perczel, A.; Foxman, B. M.; Fasman, G. D. *Proc. Natl. Acad. Sci. U.S.A.* **1992**, *89*, 8210.
- (33) Soman, K. V.; Karimi, A.; Case, D. A. *Biopolymers* **1991**, *31*, 1351.
- (34) Wright, P. E.; Dyson, H. J.; Feher, V. A.; Tennant, L. L.; Waltho, J. P.; Lerner, R. A.; Case, D. A. *Frontiers of NMR in Molecular Biology*; Patel, D., Ed.; Alan R. Liss: New York, 1990; p 1.
- (35) Tobias, D. J.; Brooks, C. L., III. *Biochemistry* **1991**, *30*, 6059.
- (36) Di Capua, F. M.; Swaminathan, S.; Beveridge, D. L. *J. Am. Chem. Soc.* **1990**, *112*, 6768.

JP950078F